

**RAID: Regression Analysis based Inductive DNA microarray for Precise Read-Across**

Yuto Amano, Masayuki Yamane, Hiroshi Honda\*

R&D Safety Science Research, Kao Corporation, 2606 Akabane, Ichikai-Machi, Haga-Gun, Tochigi,  
Japan

**\* Correspondence:**

Hiroshi Honda, Ph.D; E-mail: [honda.hiroshi@kao.com](mailto:honda.hiroshi@kao.com)

## 9 Abstract

10 Chemical structure-based read-across represents a promising method for chemical toxicity evaluation  
 11 without the need for animal testing; however, a chemical structure is not necessarily related to  
 12 toxicity. Therefore, *in vitro* studies were often used for read-across reliability refinement; however,  
 13 their external validity has been hindered by the gap between *in vitro* and *in vivo* conditions. Thus, we  
 14 developed a virtual DNA microarray, Regression Analysis based Inductive DNA microarray (RAID),  
 15 which quantitatively predicts *in vivo* gene expression profiles based on the chemical structure and/or  
 16 *in vitro* transcriptome data. For each gene, elastic-net models were constructed using chemical  
 17 descriptors and *in vitro* transcriptome data to predict *in vivo* data from *in vitro* data (*in vitro* to *in vivo*  
 18 extrapolation; IVIVE). In feature selection, useful genes for assessing the quantitative structure  
 19 activity relationship (QSAR) and IVIVE were identified. Predicted transcriptome data derived from  
 20 the RAID system reflected the *in vivo* gene expression profiles of characteristic hepatotoxic  
 21 substances. Moreover, gene ontology and pathway analyses indicated that xenobiotic response and  
 22 metabolic activation via nuclear receptors are related to those gene expressions. The identified  
 23 IVIVE-related genes were associated with fatty acid-, xenobiotic-, and drug metabolism, indicating  
 24 that *in vitro* studies were effective in evaluating these key events. Furthermore, validation studies  
 25 revealed that chemical substances associated with these key events could be detected as hepatotoxic  
 26 biosimilar substances. These results indicate that the RAID system could represent an alternative  
 27 screening test for repeated-dose toxicity test and toxicogenomic analyses. Our technology provides a  
 28 critical solution to IVIVE-based read-across by considering the mode of action and chemical  
 29 structures.

# 1 Introduction

Non-animal testing for efficacy and safety evaluation of chemical substances is one of the key concepts of balancing animal welfare and efficient development. Since the marketing ban in the EU in March 2013 ((EC) No. 1223/2009) (EU, 2009) of cosmetic products and ingredients tested on animal models, safety assessment methodologies independent of animal testing have attracted much attention. Simultaneously, the utilization of non-animal high-throughput technology for optimizing drug discovery processes is becoming highly important in pharmaceuticals (Loiodice et al., 2017; Rognan, 2017; Amano et al., 2020).

Read-across, a process that estimates substance toxicity based on the concept that substances with similar chemical structure have similar biological activity, represents a promising approach and has already been conceptually accepted as a reliable safety risk assessment by some regulatory authorities (ECHA, 2017; European Commission, 2018). Likewise, quantitative structure activity relationship (QSAR) has been widely used and impurity characterization received regulatory acceptance (ICH M7). However, since subtle structural differences may elicit different biological responses, supporting the read-across robustness by using biological similarities has been considered important (Ball et al., 2016, 2020; Zhu et al., 2016). Registration, Evaluation, Authorization, and Restriction of Chemicals (REACH) mentioned that the read-across performed by registrants often fail to comply with the legal requirements due to defects in the hypothesis and justification of the toxicological prediction (ECHA, 2020).

There are two approaches to enhance the reliability of read-across: (1) Employment of *in vitro* data relevant to specific toxicity. Methodologies to incorporate *in vitro* data within read-across (Ball et al., 2016, 2020; ECHA, 2017; Guo et al., 2019) and some case studies (OECD, 2016a, 2016b, 2018; Nakagawa et al., 2020, 2021) have been reported. However, these approaches can be applied

only to specific toxicity endpoint and substances with a known toxicity and mode of action. Such conditions were previously termed as “local validity” (Patlewicz et al., 2014). (2) The use of biologically similar substances based on their profiles obtained from a large number of bioassays. The United States Environmental Protection Agency’s (US EPA’s) research project, ToxCast and Tox21, provided hundreds of high-throughput screening assays and several groups employed such biological activity data for toxicological evaluation (Sipes et al., 2013; Berggren et al., 2015; Richard et al., 2021). Although this concept could be applied to substances with little information to elucidate their entire toxicological profiles and find their key mode of action, it is time-consuming and expensive to conduct numerous bioassays for a new candidate substance. In contrast, transcriptome data containing approximately 30,000 gene expression values can be used to estimate perturbed mechanisms through enrichment analysis. Wang et al. (2016) tried to predict drug-induced adverse effects by employing LINCS L1000 data (Subramanian et al., 2017), whereas Iwata et al. (2019) developed a computational method to predict missing value from the LINCS L1000 transcriptomic profiles of various human cell lines and provided new drug therapeutic indications. Genomic data have been considered to be usable in read-across by Health Canada and a research group from the U.S. FDA (Health Canada, 2019; Liu et al., 2019). However, several researchers showed that *in vitro* gene expression values are not always highly correlated with *in vivo* data (Sutherland et al., 2016; Grinberg et al., 2018; Liu et al., 2018). Thus, interpreting toxicological meaning from the *in vitro-in vivo* relationship and *in vitro* to *in vivo* extrapolation (IVIVE) in omics data represents a big challenge for chemical risk assessment.

As an IVIVE study in omics data, Liu et al. (2020) developed a useful *in silico* strategy to narrow the data gap between *in vitro* and *in vivo* conditions. They modified *in vitro* data using non-generative matrix factorization methods to improve the correlation with *in vivo* data, which overcame the shortcomings of previous large-scale genomic data predictions regarding the *in vitro-in vivo* data

gap (Liu et al., 2020). Although non-generative matrix factorization enables macroscopic estimation based on a pattern recognition classifying chemical and biological responses, it does not focus on each gene estimation. As an alternative solution, microscopic estimation for each gene expression were performed based on tensor-train weighted optimization using machine learning (Iwata et al., 2019); however, such comprehensive estimation have not been integrated within an IVIVE study. Therefore, predicting *in vivo* transcriptomic profiles from *in vitro* data for IVIVE might not only enhance the robustness of read-across but could also be utilized in other non-animal testing strategies as weight of evidence, such as in Integrated Approaches to Testing and Assessment (IATA) and New Approach methods (NAMs) for safety and drug repositioning research.

In this study, we developed a virtual DNA microarray that quantitatively predicts the *in vivo* gene expression profiles based on the chemical structure and/or *in vitro* transcriptome data. For each gene, elastic-net models, a regression analysis method that has been used in toxicity prediction with visualization of feature importance (e.g. Fujita et al., 2020), were constructed using chemical descriptors and *in vitro* transcriptome data. We named the set of prediction models “Regression Analysis based Inductive DNA microarray (RAID)” to inductively analyze the mode of action and the key event in adverse effects with reference to the Redundant Arrays of Inexpensive Disks, a data storage virtualization technology also represented as RAID that combines multiple physical disk drive components with the purpose of data redundancy. As RAID (storage technology) complements data based on the information of multiple components, we hope that RAID (our microarray) will complement the relationships between multiple media (*in vivo* gene expression, *in vitro* gene expression, and chemical structure). RAID system achieved the quantitative *in vitro* to *in vivo* extrapolation (QIVIVE) by the integration of a structure-based approach (QSAR) with transcriptomic data. Whereas general “Q”IVIVE studies predict dose (or concentration) quantitatively in toxicological or toxicokinetic effects, our “Q”IVIVE predicts *in vivo* gene expression values

quantitatively. Finally, the substance similarities were analyzed by principal component analysis (PCA), which proved useful in understanding the features of toxic substances based on their gene expression profile (Watanabe et al., 2012), using RAID (the virtual microarray) data, *in vivo* data, *in vitro* data, and chemical structure data to validate the usefulness of read-across.

## 2 Materials and Methods

### 2.1 Gene expression and chemical structure data

No animal experiment has been performed in this study. The transcriptome data from DNA microarrays (Affymetrix Rat Genome 230 2.0 chips; Santa Clara, CA, USA) were extracted from the Toxicogenomics Project-Genomics Assisted Toxicity Evaluation system (TG-GATEs). TG-GATEs contains *in vitro* and *in vivo* transcriptome data for rat single- and repeated-dose toxicity tests of 170 compounds (Igarashi et al., 2015). The transcriptome data obtained from the livers of rats treated with high doses for 28 days and primary rat hepatocytes treated with high doses for 24 h were downloaded and pre-processed using MAS5 (Gautier et al., 2004). In this study, chemical substances tested *in vitro* and *in vivo*, that fulfilled a maximum sample number ( $n = 2$  for *in vitro* and  $n = 3$  for *in vivo*), and had no incalculable chemical descriptors (described below), were analyzed. Thus, 115 compounds were examined in this study (Table 1).

For the chemical structure data, the alvaDesc chemical descriptors (Mauri, 2020) were calculated using alvaDesc v1.0 software (Alvascience-Srl, Lecco, Italy). AlvaDesc can calculate 3885 2D-descriptors and 1420 3D-descriptors. However, only 2D-descriptors were used excluding those with a high pair correlation ( $>0.95$ ), constant for all substances, and at least one missing value. Consequently, 854 descriptors were calculated. Each descriptor was normalized using the bestNormalize package (ver. 1.8.0) in R (ver. 4.1.1) (<https://cran.r-project.org/>). This package estimates the optimal normalizing transformation from Yeo-Johnson transformation, the Box Cox

transformation, the  $\log_{10}$  transformation, the square-root transformation, and the arcsine transformation.

## 2.2 Construction of the RAID system (a virtual microarray)

To extrapolate *in vitro* transcriptome data to *in vivo* conditions, we developed predictive models for each gene. The predictive models predicting *in vivo* transcriptome data from chemical descriptors and *in vitro* data were developed using the elastic-net regression method. The value of each cell in the matrix was the fold change on a base 2 logarithmic scale. The set of those predictive models was named a virtual microarray “RAID” (as mentioned in the Introduction) (Figure 1). To suppress over-learning, the hyperparameters ( $\alpha$  and  $\lambda$ ) of each model were optimized with a 5-fold cross-validation. We removed the genes that were associated with less than 10 chemical substances inducing differential expression ( $<1.5$  fold change) since it would be difficult to run machine learning scripts on such rare genes. Consequently, RAID was composed of 1601 prediction models for each gene.

To construct RAID that correctly predicts the bioactivities of chemical substances, the quality of training data sets was extremely important, and differentially expressed genes should be determined strictly considering data noise. Hence, we addressed this issue by data processing (feature engineering) and model justification. First, after calculating the fold change values (sample treated groups/solvent control group), the gene differentiation values with low reliability were adjusted. Briefly, the fold change value increments were changed to half (e.g. 1.5 decreased to 1.25) in the sample with the number of flag A (low reliability)  $\geq 2$  out of 3 for *in vivo* and the number of flag A  $\geq 1$  out of 2 for *in vitro*, or in the sample with p-value ranging between 0.05 and 0.1. The fold change values were changed one-fourth (e.g. 1.4 decreased to 1.1) in the sample with p-value over 0.1, and were treated as 1 (no differentiation) in the sample with flags all A in both *in vivo* and *in vitro*.

Second, weight parameters were used in model building. The weight of samples with  $\geq 1.5$  fold change was set to 1.5 and  $\geq 4$  fold change was set to 2.

### 2.3 Interpretation of biological meaning of RAID analysis

Considering the application of RAID to read-across, the gene expression data was visualized by PCA using `prcomp` function from `stats` package (ver. 4.1.1) and probability ellipse frames of toxic and non-toxic substances were drawn using the `ggfortify` package (ver. 0.4.12) in R to compare *in vivo*, *in vitro*, and chemical descriptor data. The toxic class of chemical substances were determined based on previously reported histopathological and serum chemistry findings (Table 1) (Low et al., 2011). As a reference data point, the biological meaning of genes that contributed to the PCA plot of *in vivo* data was analyzed using pathway analysis. The loading value of genes in the PCA was defined as length of loadings calculated using Pythagorean theorem

$$length = \sqrt{(loading\ of\ PC1)^2 + (loading\ of\ PC2)^2}$$

and genes with top 30 loading value in 1<sup>st</sup> and 4<sup>th</sup> quadrant were analyzed.

To analyze the biological consistency with *in vivo* data, commonality of principal component related genes (top and bottom 30 rotations in each PC1 and PC2 of PCA) were visualized using the `VennDiagram` package (ver. 1.6.20) in R, and enrichment analyses of each categorized gene were conducted using Gene Ontology-biological process and Reactome pathway by Metascape (Zhou et al., 2019). Four categorized genes related to *in vivo* data (*in vivo* only, *in vivo* and RAID, *in vivo* and *in vitro*, and all three data) were analyzed to characterize which biological process could be covered by RAID and *in vitro* data. Furthermore, to characterize genes whose predictive models in RAID used *in vitro* data, enrichment analysis of top 20 genes with the highest importance (contribution) for



*in vitro* data in the model was conducted. In the analysis, Affymetrix probe ID was converted to gene symbol using the biomaRt package (ver. 2.50.2) in R.

## 2.4 Quantitative IVIVE effects in RAID system

For performance evaluation against the quantitative IVIVE, root-mean-square errors (RMSEs) of RAID predicted values to *in vivo* data were calculated and compared to those of *in vitro* data. To exclude the difference in gene expression value distribution of each data source, fold change values were normalized before RMSEs was calculated. The RMSEs were calculated for both all genes and genes for which *in vitro* data had importance in the model.

## 2.5 Read-across application using external data

To validate the usefulness of RAID for functional read-across-based analysis of both predicted gene expression profiles and chemical structures, substances that did not contain training data sets for model building (Table 1) were further explored using Ingenuity Pathway Analysis (IPA) (QIAGEN Inc., <https://www.qiagenbioinformatics.com/products/ingenuitypathway-analysis>). Specifically, substances that may promote the expression of genes (have known relationship with the genes) that were identified by the PCA and pathway analysis of *in vivo* data (see section 2.3) were explored using IPA. Chemical descriptors of each substance were analyzed using alvaDesc v1.0 software (Alvascience-Srl, Lecco, Italy) and gene expression profiles were fulfilled using median values of training data sets. Finally, RAID analyses using constructed predictive models for those substances and re-analyzed PCA data were used to evaluate similarities based on predicted-biological responses.

# 3 Results

## 3.1 Biological analysis of RAID compared to that of *in vivo* and *in vitro* microarray data

RAID (predicted transcriptome) data was visualized using PCA (Figure 2). From a higher perspective, two directions mainly composed of toxic substances were identified and many toxic substances were separated from non-toxic substances via RAID and *in vivo* data, whereas they could not be separated based on *in vitro* and chemical descriptor data. Moreover, two common toxic-substances groups (e.g. 1<sup>st</sup> group [TAA, MP, and HCB] placed in 1<sup>st</sup> quadrant and 2<sup>nd</sup> group [WY, FFB, BBr, and GFZ] placed in 2<sup>nd</sup> quadrant) were distanced from non-toxic substances along PC1 and PC2 in both RAID and *in vivo* data, nonetheless the PC1 and PC2 replaced. The loading plot showed that *Cyp1a1* (Cytochrome P450, family 1, subfamily A, polypeptide 1), *Gpx2* (Glutathione peroxidase 2), and *Gsta3* (Glutathione S-transferase A3) gene expression were commonly observed in RAID and *in vivo* data, and enabled the discrimination of TAA, MP, and HCB. Furthermore, *Acot1* (Acyl-CoA thioesterase 1), *Vnn1* (Vanin1), and *Cyp4a11* (Cytochrome P450, family 4, subfamily A, polypeptide 11) contributed to discriminating WY, FFB, BBr, and GFZ.

Pathway analysis indicated that the 1<sup>st</sup> group related genes would be associated with peroxisome proliferative activity characterized by *Cyp4a* induction via peroxisome proliferator-activated receptor-alpha (PPARα) activation and 2<sup>nd</sup> group related genes would be associated with xenobiotic response, including *Cyp1a* induction via aryl hydrocarbon receptor (AHR) and carcinogenesis (Figure 3). To clarify the biological functions that RAID covers, the commonalities between related genes and principal components were explored (Figure 4A and Table 2). As expected from Figure 2, RAID shared more genes (36; Table 2) with the *in vivo* data than with the *in vitro* data (9). Enrichment analysis revealed that the biological processes related to metabolism and detoxification and pathways associated with peroxisomal protein transport were enriched in both *in vivo* and RAID data, indicating that RAID could cover these functions, and ultimately indicate key functions through pathway analysis (Figure 3). Conversely, although several metabolic processes were enriched within the *in vitro* data, those biological functions were covered by RAID as well

(Figure 4B). These results suggest that RAID data allow the detection of more *in vivo* key toxic events than *in vitro* transcriptome data.

### 3.2 Importance of *in vitro* data in the RAID system

Enrichment analysis of genes whose predictive model used highly relevant *in vitro* data (top 20 genes for which *in vitro* data had high importance in all predictive models; Table 3) indicated that *in vitro* data contributed to estimating the gene expression values associated with metabolic processes of fatty acid, xenobiotics, and drugs, and peroxisome proliferative activity (Pathway on peroxisome protein import and biological process associated with the regulation of peroxisome size; Figure 5).

### 3.3 Quantitative IVIVE performance in the RAID system

To evaluate the RAID performance in terms of gene expression value, RMSEs were calculated for all genes and the genes for which *in vitro* data had importance in predictive models. Considering RAID would be used in read-across, we compared the RMSEs of RAID data to that of *in vitro* data, which was conventional non-animal test approaches (Figure 6). As a result, RMSEs decreased in RAID, indicating a better performance than what could be obtained using *in vitro* data.

### 3.4 Validation of prediction models using external data

In PCA using *in vivo* and RAID data as well as the pathway analysis of PC related genes (Figure 2 and 3), genes related to peroxisome proliferative activity and xenobiotic metabolism activity possibly leading to liver cancer, which were respectively characterized by *Cyp4* induction via PPARa and *Cyp1a* induction via AHR, were identified as key features. Thus, potential *Cyp4a*- and *Cyp1a*-inducers were explored using the knowledge-based approach using the IPA software. Moreover, using the top 30 genes identified using PCA (described in 2.3 section), upstream regulator analysis focusing on chemical substances was performed and 20 chemicals were identified. Finally, a total of

21 chemicals (potential *Cyp1a* inducers: 10 chemicals, potential *Cyp4a* inducers: 11 chemicals) were selected as candidates for external validation and subjected to RAID analyses (Table 4). Substances already present in the TG-GATE (training sets) or had uncalculated chemical descriptors data were excluded.

For the PCA analysis, approximately half of the substances were plotted with positive PC scores, which is in consistence with the direction expected from the training data set for both potential *Cyp1a*- and *Cyp4a*-inducers (Figure 7). Lastly, pentachlorobiphenyl, polychlorinated biphenyls, and pentachlorodibenzofuran were isolated as *Cyp1a*-inducers, whereas nafenopin, ciprofibrate, and di(2-ethylhexyl) phthalate were isolated as *Cyp4a*-inducers.

## 4 Discussions

The transcriptome data signatures derived from RAID (the virtual microarray) system were in good agreement with those of *in vivo* data, and the technology provided an understanding of the features of hepatotoxic substances based on the toxicological mechanism interpretation. The mechanism of action of the two characteristic toxic substances separated using PCA analysis was shown to be achieved through *Cyp4a* induction via PPARa and *Cyp1a* induction via AHR (pathway and gene ontology analysis). The PPARa-induced drug toxicity requires species differentiation considerations (Ito et al., 2006) and AHR-induced drugs raise safety concerns during developmental periods (Qin et al., 2019). Therefore, predicting the involvement of these nuclear receptors and induction of metabolic enzymes is critical for understanding the molecular initiating events and the key events associated with adverse outcome pathway. RAID enables the prediction of gene expression levels; thus, exhibiting properties required for next generation risk assessment methods.

The 1<sup>st</sup> substance group (TAA, MP, and HCB), representing toxic substances commonly differentiated from non-toxic substances using PCA on *in vivo* and RAID data, has been reported to have carcinogenicity with metabolic activation (Uehara et al., 2008; Hajovsky et al., 2012; US. HSS., 2015). Furthermore, they have been shown to activate xenobiotic related receptors, such as AHR inducing *Cyp1a* (Ushel et al., 2002; Yamashita et al., 2014; Clara et al., 2015). Moreover, *in vivo* transcriptome data in this study showed that TAA, MP, and HCP induce *Cyp1a* activation. AHR is known for mediating the toxicity and tumor promoting properties despite the mechanism through which AHR activates carcinogenesis remains to be elucidated (Safe et al., 2013; Murray et al., 2014).

The 2<sup>nd</sup> substance group (WY, FFB, BBr, and GFZ) includes fibrates which are recognized as PPARa agonists (Schoonjans et al., 1996), implying that induction of *Cyp4a* via PPARa and perturbation of lipid-related genes are involved as a series of key events. Although another fibrate

included in training data, clofibrate (CFB), was classified as a non-toxic substance according to no serum chemistry findings from a previous study, CFB was shown to act as a PPAR $\alpha$  agonist inducing peroxisomal proliferation on hepatocyte (Low et al., 2011) and was plotted around the 2<sup>nd</sup> group in PCA. Sustained activation of PPAR $\alpha$  signaling and induction of enzymes, such as CYP4A, to increased fatty acid oxidation contributes to sustained oxidative stress in liver. These changes lead to liver cell damage as hypertrophy and proliferation which contribute to the development of hepatocellular carcinomas (Parimal et al., 2013).

From the perspective of capturing individual gene responses, RAID was able to detect gene expressions related to major drug metabolism responses in *in vivo* more broadly (more common principal component related gene number; Figure 4) and quantitatively (less RMSE value; Figure 6) than *in vitro*. The 36 genes that were commonly related to principal components of *in vivo* and RAID data contained genes that were known to be involved in drug metabolism and hepatotoxicity. In addition to the genes described above (*Cyp1a* and *Cyp4a*), *Acot1* acts as an auxiliary enzyme in the oxidation process of various lipids in peroxisomes (Hunt et al., 2012). Furthermore, *Vnn1* is expressed by the centrilobular hepatocytes and is involved in lipid and xenobiotic metabolism (Bartucci et al., 2019), whereas *Pex11a* (*Peroxisomal biogenesis factor 11 alpha*) is involved in peroxisome maintenance and proliferation associated with dyslipidemia (Chen et al., 2018). All of these genes are known as PPAR $\alpha$  target genes (Rakhshandehroo et al., 2010; Lake et al., 2016). Thus, these features indicate that RAID can predict possible toxicity by taking into account a broader range of mechanisms than the range of *in vitro* data. Indeed, the *in vivo* changes detected using the *in vitro* data were limited (Figure 4), and the PCA showed most of the differentially expressed genes were associated with irrelevant non-physiological conditions. Thus, the IVIVE effect combining QSAR technique and *in vitro* data would allow for more precise predictions through denoising this type of *in vitro* specific biological responses.

*In vitro* data contribute to accurate gene expression predictions that could not be achieved with QSAR alone (Figure 2D). *In vitro* data contributed to the prediction of the mechanism shown in Figure 5. The biological mechanisms related to metabolic processes were consistent with the key mechanisms of characteristic hepatotoxic substances described above, which indicates that *in vitro* data contributes to the precise predictions obtained using RAID. In addition, whether *in vitro* responses were observed in the suggested mode of action predicted by the RAID system or not is an important point in term of weight of evidence. This study provides valuable evidence supporting that transcriptome data should be considered in light of previous reports indicating that *in vitro* data does not necessarily reflect *in vivo* conditions (Tamura et al., 2006; Sutherland et al., 2016). Simultaneously, *in vitro* studies focusing on a specific mechanism should consider the external validity of their findings and whether the findings reflect *in vivo* situations.

Evaluating the read-across performance using external substances, such as 3,4,5,3',4'-pentachlorobiphenyl, 2,2',4,4'-tetrachlorobiphenyl (a type of polychlorinated biphenyl) and pentachlorodibenzofuran (dioxin-like compounds) (Figure 7A), which are known as IARC group 1 carcinogens and *Cyp1a1* inducers (EPA, 1996; Walker et al., 2005; National Toxicology Program, 2006), were separated as toxic-substances. Additionally, benzo(a)pyrene, 3-methylcholanthrene, and 9,10-dimethyl-1,2-benzanthracene plotted apart from origin of coordinates (PC1 = 0 and PC2 = 0) and are polycyclic aromatic hydrocarbons inducing *Cyp1a1* (Moorthy et al., 2007; Pushparajah et al., 2008). Non-carcinogenic chemical substances, such as foods components or preservatives, were positioned near the origin, second quadrant or third quadrant, indicating low risk. Furthermore, substances interacting with *Cyp4a* (Figure 7B), such as ciprofibrate, nafenopine, clofenapate, clofibrac acid, and di(2-ethylhexyl) phthalate, which are plotted in the area of the 2<sup>nd</sup> substance group (PC1 > 0), are also known as PPARα agonist (Bocos et al., 1995; Roberts et al., 2002; Yadetie et al., 2003; Currie et al., 2005; Pyper et al., 2010). Chemicals that were not characterized by the PC1

component ( $PC1 < 0$ ) are not hyperlipidemia drugs. These results suggest that the RAID system effectively classifies substances that based on the mode of action as well as the strength of toxicity, and ultimately contributes to precise read-across. Thus, the RAID system provides a new method for read-across in line with IATA that should be called “a virtual functional read-across”. Here, we showed that compounds without high structural similarities might have similar toxicological properties, and our new approach interpreted the shared mechanism of action. This means that RAID considers the qualitative and quantitative similarities of biological responses, which was one of the major issues of QSAR-based read-across. The structural similarities of TAA, MP, and HCB observe using correlation coefficient of the chemical descriptor used for the predictive model and the maximum common substructure (MCS) similarities with the Tanimoto coefficient is less than 0.5; however, the homology of RAID and *in vivo* data is as high as 0.8. Furthermore, achieving such an accurate read-across without using *in vitro* data will provide a new perspective on the structural information-based predictions.

PCA analysis was used to understand the features of substances to predict the modes of action and identify biologically similar compounds for read-across in this study. Hence, focusing on certain specific toxicity, discriminant analysis, classifier model, or biomarker analysis might improve the separation of toxic substances. Indeed, the use of RAID data instead of experimental transcriptome data would achieve previously reported biomarker-based classification without using animals. For example, Liu et al. (2017) indicated that certain genes associated with hepatocellular hypertrophy and hepato-carcinogenesis, and markers, such as *Cyp1a1*, *Acot1*, *Stac3* (*SH3 and cysteine rich domain 3*), and *Hdc* (*Histidine decarboxylase*), which were correctly evaluated in the present study to characterize hepatotoxic compounds in PCA. Similarly, the constructed RAID system could be applied to previous studies to predict carcinogenicity or estimate transcriptional benchmark dose by



toxicogenomics analysis of short term *in vivo* studies (Ellinger-ziegelbauer et al., 2008; Thomas et al., 2013; Matsumoto et al., 2014; Kawamoto et al., 2017).

One important issue that should be considered in toxicological evaluation using the RAID system is consideration of species differences. The RAID system provides mechanistic insights on repeated-dose toxicity in animal models; however, since some species differences have observed, the suggested mode of action and the corresponding molecules need to be confirmed by toxicologists. Moreover, evaluation on RAID usefulness for various toxicities is required.

The present approach integrates QSAR and IVIVE and will contribute to other areas of research, such as drug repositioning, which recently attracted attentions towards pharmaceuticals that are available on the market and might be repurposed for new diseases (Jourdan et al., 2020). However, the previously proposed methodologies (Iwata et al., 2018; Lippmann et al., 2018; Zhu et al., 2020; He et al., 2021) have a room for improving the IVIVE aspect of *in vivo* prediction. Thus, our system provides an alternative to screen candidate drugs and explore new biologically similar drugs at a low cost.

In conclusion, we developed a virtual DNA microarray system that quantitatively predicts *in vivo* gene expression profiles based on the chemical structure and/or *in vitro* transcriptome data. Estimated transcriptomes are considered scientifically relevant from PCA data interpretation as well as pathway and GO analysis. Based on its external validation, our system works as an alternative test for repeated dose toxicity tests with toxicogenomic analysis enabling IVIVE and mechanism estimation. Although our technology might have limited applicability domain due to the small data size of chemical substances and their characteristic (using hepatotoxic substances), the concept of the virtual microarray analysis contributes to 3Rs and might benefit every future animal testing.

## 5 Conflict of Interest

*The authors declare that the research was conducted in the absence of any commercial or financial relationships that could be construed as a potential conflict of interest.*

## **6 Author Contributions**

YA and HH contributed to conception and design of the study. YA and HH constructed in silico models, performed enrichment analyses, interpret the biological meanings of the models, and contributed to statistical analyses. HH collected the datasets from TG-GATE. HH and MY supervised this project. YA and HH drafted the manuscript. All authors contributed to manuscript writing, confirmed the final version of the manuscript, and agreed to the contents.

## **7 Funding**

This research received no external funding.

## **8 Acknowledgments**

We thank Dr. Osamu Morita, Dr. Kaede Miyata, and Mr. Yasuaki Inoue for their helpful suggestions and valuable discussions to the present study.

## **9 References**

- Amano, Y., Honda, H., Sawada, R., Nukada, Y., Yamane, M., Ikeda, N., et al. (2020). In silico systems for predicting chemical-induced side effects using known and potential chemical protein interactions, enabling mechanism estimation. *J. Toxicol. Sci.* 45, 137–149. doi:10.2131/jts.45.137.
- Ball, N., Cronin, M. T. D., Shen, J., Blackburn, K., Booth, E. D., Bouhifd, M., et al. (2016). Toward Good Read-Across Practice (GRAP) Guidance. *ALTEX* 33, 149–166.

381 Ball, N., Madden, J., Paini, A., Mathea, M., Palmer, A. D., Sperber, S., et al. (2020). Key read across  
382 framework components and biology based improvements. *Mutat. Res. Gen. Tox. En.* 853,  
383 503172. doi:10.1016/j.mrgentox.2020.503172.

384 Bartucci, R., Salvati, A., and Olinga, P. (2019). Vanin 1 : Its physiological function and role in  
385 diseases. *Int. J. Mol. Sci.* 20, 3891.

386 Berggren, E., Amcoff, P., Benigni, R., Blackburn, K., Carney, E., Cronin, M., et al. (2015). Chemical  
387 safety assessment using read-across: Assessing the use of novel testing methods to strengthen  
388 the evidence base for decision making. *Environ. Health Perspect.* 123, 1232–1240.  
389 doi:10.1289/ehp.1409342.

390 Bocos, C., Gttlicher, M., Gearing, K., Banner, C., Enmark, E., Teboul, M., et al. (1995). Fatty acid  
391 activation of peroxisome proliferator-activated receptor (PPAR). *J. Steroid Biochem. Molec.*  
392 *Biol.* 53, 467–473.

393 Chen, C., Wang, H., Chen, B., Chen, D., Lu, C., Li, H., et al. (2018). Pex11a deficiency causes  
394 dyslipidaemia and obesity in mice. *J. Cell. Mol. Med.* 23, 2020–2031. doi:10.1111/jcmm.14108.

395 Clara, A., Portaz, D. T., Caimi, G. R., Sánchez, M., Chiappini, F., Randi, A. S., et al. (2015).  
396 Hexachlorobenzene induces cell proliferation, and aryl hydrocarbon receptor expression (AhR)  
397 in rat liver preneoplastic foci, and in the human hepatoma cell line HepG2. AhR is a mediator of  
398 ERK1 / 2 signaling, and cell cycle regulation in HCB-treated HepG. *Toxicology* 336, 36–47.  
399 doi:10.1016/j.tox.2015.07.013.

400 Currie, R. A., Bombail, V., Oliver, J. D., Moore, D. J., Lim, F. L., Gwilliam, V., et al. (2005). Gene  
401 ontology mapping as an unbiased method for identifying molecular pathways and processes

402 affected by toxicant exposure: Application to acute effects caused by the rodent non-genotoxic  
 403 carcinogen diethylhexylphthalate. *Toxicol. Sci.* 86, 453–469. doi:10.1093/toxsci/kfi207.

404 ECHA (2017). Read-Across Assessment Framework (RAAF). doi:10.2823/619212.

405 ECHA (2020). The Use of Alternatives to Testing on Animals for the REACH Regulation.  
 406 doi:10.2823/092305.

407 Ellinger-ziegelbauer, H., Gmuender, H., Bandenburg, A., and Juergen, H. (2008). Prediction of a  
 408 carcinogenic potential of rat hepatocarcinogens using toxicogenomics analysis of short-term in  
 409 vivo studies. *Mutat. Res.* 637, 23–39. doi:10.1016/j.mrfmmm.2007.06.010.

410 EPA, U. S. (1996). PCBs : Cancer Dose-Response Assessment and Application to Environmental  
 411 Mixtures.

412 EU (2009). Regulation (EC) no. 1223/2009 of the European parliament and of the council of 30  
 413 November 2009 on cosmetics products. *Off. J. Eur. Union* L 342, 59–209.

414 European Commission (2018). The SCCS Notes of Guidance for the Testing of Cosmetic Ingredients  
 415 and their Safety Evaluation 10th revision.  
 416 [https://ec.europa.eu/health/sites/health/files/scientific\\_committees/consumer\\_safety/docs/sccs\\_o](https://ec.europa.eu/health/sites/health/files/scientific_committees/consumer_safety/docs/sccs_o)  
 417 [\\_224.pdf](https://ec.europa.eu/health/sites/health/files/scientific_committees/consumer_safety/docs/sccs_o_224.pdf) [Accessed February 14, 2022].

418 Fujita, Y., Morita, O., and Honda, H. (2020). In silico model for chemical-induced chromosomal  
 419 damages elucidates mode of action and irrelevant positives. *Genes (Basel)*. 11, 1181.

420 Gautier, L., Cope, L., Bolstad, B. M., and Irizarry, R. A. (2004). Affy - Analysis of Affymetrix  
 421 GeneChip data at the probe level. *Bioinformatics* 20, 307–315.  
 422 doi:10.1093/bioinformatics/btg405.

423 Grinberg, M., Stöber, R. M., Albrecht, W., Edlund, K., Schug, M., Godoy, P., et al. (2018).  
 424 Toxicogenomics directory of rat hepatotoxicants in vivo and in cultivated hepatocytes. *Arch.*  
 425 *Toxicol.* 92, 3517–3533. doi:10.1007/s00204-018-2352-3.

426 Guo, Y., Zhao, L., Zhang, X., and Zhu, H. (2019). Using a hybrid read-across method to evaluate  
 427 chemical toxicity based on chemical structure and biological data. *Ecotoxicol. Environ. Saf.* 178,  
 428 178–187. doi:10.1016/j.ecoenv.2019.04.019.

429 Hajovsky, L., Hu, G., Koen, Y., Sarma, D., Cui, W., Moore, D. S., et al. (2012). Metabolism and  
 430 toxicity of thioacetamide and thioacetamide S-Oxide in rat hepatocytes. *Chem. Res. Toxicol.* 25,  
 431 1955–1963. doi:10.1021/tx3002719.

432 He, B., Hou, F., Ren, C., Bing, P., and Xiao, X. (2021). A review of current in silico methods for  
 433 repositioning drugs and chemical compounds. *Front. Oncol.* 11, 711225.  
 434 doi:10.3389/fonc.2021.711225.

435 Health Canada (2019). Evaluation of the Use of Toxicogenomics in Risk Assessment at Health  
 436 Canada: An Exploratory Document on Current Health Canada Practices for the Use of  
 437 Toxicogenomics in Risk Assessment. [https://www.canada.ca/en/health-](https://www.canada.ca/en/health-canada/services/publications/science-research-data/evaluation-use-toxicogenomics-risk-assessment.html)  
 438 [canada/services/publications/science-research-data/evaluation-use-toxicogenomics-risk-](https://www.canada.ca/en/health-canada/services/publications/science-research-data/evaluation-use-toxicogenomics-risk-assessment.html)  
 439 [assessment.html](https://www.canada.ca/en/health-canada/services/publications/science-research-data/evaluation-use-toxicogenomics-risk-assessment.html) [Accessed February 14, 2022].

440 Hunt, M. C., Siponen, M. I., and Alexson, S. E. H. (2012). The emerging role of acyl-CoA  
 441 thioesterases and acyltransferases in regulating peroxisomal lipid metabolism. *Biochim.*  
 442 *Biophys. Acta* 1822, 1397–1410. doi:10.1016/j.bbadis.2012.03.009.

443 Igarashi, Y., Nakatsu, N., Yamashita, T., Ono, A., Ohno, Y., Urushidani, T., et al. (2015). Open TG-  
444 GATEs: A large-scale toxicogenomics database. *Nucleic Acids Res.* 43, D921–D927.  
445 doi:10.1093/nar/gku955.

446 Ito, O., Nakamura, Y., Tan, L., Ishizuka, T., Sasaki, Y., Minami, N., et al. (2006). Expression of  
447 cytochrome P-450 4 enzymes in the kidney and liver : Regulation by PPAR and species-  
448 difference between rat and human. *Mol. Cell. Biochem.* 284, 141–148. doi:10.1007/s11010-005-  
449 9038-x.

450 Iwata, M., Hirose, L., Kohara, H., Liao, J., Sawada, R., Akiyoshi, S., et al. (2018). Pathway-based  
451 drug repositioning for cancers: computational prediction and experimental validation. *J. Med.*  
452 *Chem.* 61, 9583–9595. doi:10.1021/acs.jmedchem.8b01044.

453 Iwata, M., Yuan, L., Zhao, Q., Tabei, Y., Berenger, F., Sawada, R., et al. (2019). Predicting drug-  
454 induced transcriptome responses of a wide range of human cell lines by a novel tensor-train  
455 decomposition algorithm. *Bioinformatics* 35, i191–i199. doi:10.1093/bioinformatics/btz313.

456 Jourdan, J. P., Bureau, R., Rochais, C., and Dallemagne, P. (2020). Drug repositioning: a brief  
457 overview. *J. Pharm. Pharmacol.* 72, 1145–1151. doi:10.1111/jphp.13273.

458 Kawamoto, T., Ito, Y., Morita, O., and Honda, H. (2017). Mechanism-based risk assessment strategy  
459 for drug-induced cholestasis using the transcriptional benchmark dose derived by  
460 toxicogenomics. *J. Toxicol. Sci.* 42, 427–436.

461 Lake, A. D., Wood, C. E., Bhat, V. S., Chorley, B. N., Carswell, G. K., Sey, Y. M., et al. (2016).  
462 Dose and effect thresholds for early key events in a PPARα-mediated mode of action. *Toxicol.*  
463 *Sci.* 149, 312–325. doi:10.1093/toxsci/kfv236.

464 Lippmann, C., Kringel, D., Ultsch, A., and Lötsch, J. (2018). Computational functional genomics-  
465 based approaches in analgesic drug discovery and repurposing. *Pharmacogenomics* 19, 783–  
466 797. doi:10.2217/pgs-2018-0036.

467 Liu, S., Kawamoto, T., Morita, O., Yoshinari, K., and Honda, H. (2017). Discriminating between  
468 adaptive and carcinogenic liver hypertrophy in rat studies using logistic ridge regression  
469 analysis of toxicogenomic data: The mode of action and predictive models. *Toxicol. Appl.*  
470 *Pharmacol.* 318, 79–87. doi:10.1016/j.taap.2017.01.006.

471 Liu, Y., Jing, R., Wen, Z., and Li, M. (2020). Narrowing the gap between in vitro and in vivo genetic  
472 profiles by deconvoluting toxicogenomic data in silico. *Front. Pharmacol.* 10, 1489.  
473 doi:10.3389/fphar.2019.01489.

474 Liu, Z., Delavan, B., Roberts, R., and Tong, W. (2018). Transcriptional responses reveal similarities  
475 between preclinical rat liver testing systems. *Front. Genet.* 9, 1–10.  
476 doi:10.3389/fgene.2018.00074.

477 Liu, Z., Huang, R., Roberts, R., and Tong, W. (2019). Toxicogenomics: A 2020 vision. *Trends*  
478 *Pharmacol. Sci.* 40, 92–103. doi:10.1016/j.tips.2018.12.001.

479 Loiodice, S., Nogueira da Costa, A., and Atienzar, F. (2017). Current trends in in silico, in vitro  
480 toxicology, and safety biomarkers in early drug development. *Drug Chem. Toxicol.* 42, 1–9.  
481 doi:10.1080/01480545.2017.1400044.

482 Low, Y., Uehara, T., Minowa, Y., Yamada, H., Ohno, Y., Urushidani, T., et al. (2011). Predicting  
483 drug-induced hepatotoxicity using QSAR and toxicogenomics approaches. *Chem. Res. Toxicol.*  
484 24, 1251–1262. doi:10.1021/tx200148a.

485 Matsumoto, H., Saito, F., and Takeyoshi, M. (2014). CARCINOscreen ® : New short-term prediction  
486 method for hepatocarcinogenicity of chemicals based on hepatic transcript profile in rats. *J.*  
487 *Toxicol. Sci.* 39, 725–734.

488 Mauri, A. (2020). “alvaDesc: A tool to calculate and analyze molecular descriptors and fingerprints,”  
489 in Roy K. (eds) *Ecotoxicological QSARs. Methods in Pharmacology and Toxicology*. (Humana,  
490 New York, NY), 801–820. doi:10.1007/978-1-0716-0150-1\_32.

491 Moorthy, B., Muthiah, K., Fazili, I. S., Kondraganti, S. R., Wang, L., Couroucli, X. I., et al. (2007).  
492 3-Methylcholanthrene elicits DNA adduct formation in the CYP1A1 promoter region and  
493 attenuates reporter gene expression in rat H4IIE cells. *Biochem. Biophys. Res. Commun.* 354,  
494 1071–1077. doi:10.1016/j.bbrc.2007.01.103.

495 Murray, I. A., Patterson, A. D., and Perdew, G. H. (2014). Aryl hydrocarbon receptor ligands in  
496 cancer: Friend and foe. *Nat. Rev. Cancer* 14, 801–814. doi:10.1038/nrc3846.

497 Nakagawa, S., Okamoto, M., Nukada, Y., and Morita, O. (2020). Comparison of the potential  
498 mechanisms for hepatotoxicity of p -dialkoxy chlorobenzenes in rat primary hepatocytes for  
499 read-across. *Regul. Toxicol. Pharmacol.* 113, 104617. doi:10.1016/j.yrtph.2020.104617.

500 Nakagawa, S., Okamoto, M., Yoshihara, K., Nukada, Y., and Morita, O. (2021). Grouping of  
501 chemicals based on the potential mechanisms of hepatotoxicity of naphthalene and structurally  
502 similar chemicals using in vitro testing for read-across and its validation. *Regul. Toxicol.*  
503 *Pharmacol.* 121, 104874. doi:10.1016/j.yrtph.2021.104874.

504 National Toxicology Program (2006). NTP toxicology and carcinogenesis studies of 3, 3', 4, 4', 5-  
505 pentachlorobiphenyl (PCB 126)(CAS No. 57465-28-8) in female Harlan Sprague-Dawley rats  
506 (Gavage Studies). *Natl. Toxicol. Program. Tech. Rep. Ser.* 520, 4–426.



507 OECD (2016a). Case study on the use of an integrated approach to testing and assessment for  
508 hepatotoxicity of allyl esters (Series on Testing and Assessment No. 253). 1–33.  
509 [https://www.oecd.org/officialdocuments/publicdisplaydocumentpdf/?cote=env/jm/mono\(2016\)5](https://www.oecd.org/officialdocuments/publicdisplaydocumentpdf/?cote=env/jm/mono(2016)5)  
510 1&doclanguage=en [Accessed February 14, 2022].

511 OECD (2016b). Case study on the use of integrated approaches for testing and assessment for in vitro  
512 mutagenicity of 3,3' dimethoxybenzidine (DMOB) based direct dyes (Series on Testing and  
513 Assessment No. 251). 1–49.  
514 [https://www.oecd.org/officialdocuments/publicdisplaydocumentpdf/?cote=env/jm/mono\(2016\)4](https://www.oecd.org/officialdocuments/publicdisplaydocumentpdf/?cote=env/jm/mono(2016)4)  
515 9&doclanguage=en [Accessed February 14, 2022].

516 OECD (2018). Case study on grouping and read-across for nanomaterials — genotoxicity of nano-  
517 TiO<sub>2</sub> (Series on Testing and Assessment No. 292). 1–56.  
518 [https://www.oecd.org/officialdocuments/publicdisplaydocumentpdf/?cote=ENV/JM/MONO\(20](https://www.oecd.org/officialdocuments/publicdisplaydocumentpdf/?cote=ENV/JM/MONO(20)  
519 18)28&docLanguage=En [Accessed February 14, 2022].

520 Parimal, M., Navin, V., and Janardan K, R. (2013). “Peroxisome Proliferator-Activated Receptor- $\alpha$   
521 Signaling in Hepatocarcinogenesis” in Peroxisomes and their Key Role in Cellular Signaling  
522 and Metabolism (Vol. 69), ed L. A. del Río (Dordrecht, Springer). <http://doi.org/10.1007/978->  
523 94-007-6889-5.

524 Patlewicz, G., Ball, N., Becker, R. A., Booth, E. D., Cronin, M. T. D., Kroese, D., et al. (2014).  
525 Read-across approaches - Misconceptions, promises and challenges ahead. *ALTEX* 31, 387–396.  
526 doi:10.14573/altex.1410071.

527 Pushparajah, D. S., Umachandran, M., Nazir, T., Plant, K. E., Plant, N., Lewis, D. F. V., et al. (2008).  
528 Up-regulation of CYP1A / B in rat lung and liver , and human liver precision-cut slices by a

529 series of polycyclic aromatic hydrocarbons ; association with the Ah locus and importance of  
530 molecular size. *Toxicol. Vitr.* 22, 128–145. doi:10.1016/j.tiv.2007.08.014.

531 Pyper, S. R., Viswakarma, N., Yu, S., and Reddy, J. K. (2010). PPAR $\alpha$ : Energy combustion,  
532 hypolipidemia, inflammation and cancer. *Nucl. Recept. Signal.* 8, e002. doi:10.1621/nrs.08002.

533 Qin, C., Aslamkhan, A. G., Pearson, K., Tanis, K. Q., Podtelezhnikov, A., Frank, E., et al. (2019).  
534 AhR activation in pharmaceutical development: Applying liver gene expression biomarker  
535 thresholds to identify doses associated with tumorigenic risks in rats. *Toxicol. Sci.* 171, 46–55.  
536 doi:10.1093/toxsci/kfz125.

537 Rakhshandehroo, M., Knoch, B., Michael, M., and Kersten, S. (2010). Peroxisome proliferator-  
538 activated receptor alpha target genes. *PPAR Res.* 2010. doi:10.1155/2010/612089.

539 Richard, A. M., Huang, R., Waidyanatha, S., Shinn, P., Collins, B. J., Thillainadarajah, I., et al.  
540 (2021). The Tox21 10K compound library: Collaborative chemistry advancing toxicology.  
541 *Chem. Res. Toxicol.* 34, 189–216. doi:10.1021/acs.chemrestox.0c00264.

542 Roberts, R. A., Chevalier, S., Hasmall, S. C., James, N. H., Cosulich, S. C., and Macdonald, N.  
543 (2002). PPAR alpha and the regulation of cell division and apoptosis. *Toxicology* 181–182, 167–  
544 70. doi:10.1016/s0300-483x(02)00275-5.

545 Rognan, D. (2017). The impact of in silico screening in the discovery of novel and safer drug  
546 candidates. *Pharmacol. Ther.* 175, 47–66. doi:10.1016/j.pharmthera.2017.02.034.

547 Safe, S., Lee, S. O., and Jin, U. H. (2013). Role of the aryl hydrocarbon receptor in carcinogenesis  
548 and potential as a drug target. *Toxicol. Sci.* 135, 1–16. doi:10.1093/toxsci/kft128.

549 Schoonjans, K., Staels, B., and Auwerx, J. (1996). Role of the peroxisome proliferator-activated  
550 receptor (PPAR) in mediating the effects of fibrates and fatty acids on gene expression. *J. Lipid*  
551 *Res.* 37, 907–925. doi:10.1016/S0022-2275(20)42003-6.

552 Sipes, N. S., Martin, M. T., Kothiya, P., Reif, D. M., Judson, R. S., Richard, A. M., et al. (2013).  
553 Profiling 976 ToxCast chemicals across 331 enzymatic and receptor signaling assays. *Chem.*  
554 *Res. Toxicol.* 26, 878–895. doi:10.1021/tx400021f.

555 Subramanian, A., Narayan, R., Corsello, S. M., Peck, D. D., Natoli, T. E., Lu, X., et al. (2017). A  
556 next generation Connectivity Map: L1000 platform and the first 1,000,000 profiles. *Cell* 171,  
557 1437-1452.e17. doi:10.1016/j.cell.2017.10.049.

558 Sutherland, J. J., Jolly, R. A., Goldstein, K. M., and Stevens, J. L. (2016). Assessing concordance of  
559 drug-induced transcriptional response in rodent liver and cultured hepatocytes. *PLoS Comput.*  
560 *Biol.* 12, 1–31. doi:10.1371/journal.pcbi.1004847.

561 Tamura, K., Ono, A., Miyagishima, T., Nagao, T., and Urushidani, T. (2006). Profiling of gene  
562 expression in rat liver and rat primary cultured hepatocytes treated with peroxisome  
563 proliferators. *J. Toxicol. Sci.* 31, 471–490. doi:10.2131/jts.31.471.

564 Thomas, R. S., Wesselkamper, S. C., Wang, N. C. Y., Zhao, Q. J., Petersen, D. D., Lambert, J. C., et  
565 al. (2013). Temporal concordance between apical and transcriptional points of departure for  
566 chemical risk assessment. *Toxicol. Sci.* 134, 180–194. doi:10.1093/toxsci/kft094.

567 Uehara, T., Kiyosawa, N., Hirode, M., Omura, K., Shimizu, T., Ono, A., et al. (2008). Gene  
568 expression profiling of methapyrilene-induced hepatotoxicity in rat. *J. Toxicol. Sci.* 33, 37–50.  
569 doi:10.2131/jts.33.37.

570 US. HSS. (2015). Toxicological Profile for Hexachlorobenzene. doi:10.1201/9781420061888\_ch20.

571 Ushel, P. I. R. B., Toll, R. A. S., Lanchard, K. E. B., Ayadev, S. U. J., Ennant, R. A. W. T.,  
572 Unningham, M. I. L. C., et al. (2002). Methapyrilene toxicity : anchorage of pathologic  
573 observations to gene expression alterations. *Toxicol. Pathol.* 30, 470–482.  
574 doi:10.1080/01926230290105712.

575 Walker, N. J., Crockett, P. W., Nyska, A., Brix, A. E., Jokinen, M. P., Sells, D. M., et al. (2005).  
576 Dose-additive carcinogenicity of a defined mixture of “dioxin-like compounds.” *Environ.*  
577 *Health Perspect.* 113, 43–48. doi:10.1289/ehp.7351.

578 Wang, Z., Clark, N. R., and Ma’ayan, A. (2016). Drug-induced adverse events prediction with the  
579 LINCS L1000 data. *Bioinformatics* 32, 2338–2345. doi:10.1093/bioinformatics/btw168.

580 Watanabe, T., Suzuki, T., Natsume, M., and Nakajima, M. (2012). Discrimination of genotoxic and  
581 non-genotoxic hepatocarcinogens by statistical analysis based on gene expression profiling in  
582 the mouse liver as determined by quantitative real-time PCR. *Mutat. Res.* 747, 164–175.  
583 doi:10.1016/j.mrgentox.2012.04.011.

584 Yadetie, F., Laegreid, A., Bakke, I., Kusnierczyk, W., Komorowski, J., Waldum, H. L., et al. (2003).  
585 Liver gene expression in rats in response to the peroxisome proliferator-activated receptor- $\alpha$   
586 agonist ciprofibrate. *Physiol. Genomics* 15, 9–19. doi:10.1152/physiolgenomics.00064.2003.

587 Yamashita, Y., Ueyama, T., Nishi, T., Yamamoto, Y., and Kawakoshi, A. (2014). Nrf2-inducing  
588 anti-oxidation stress response in the rat liver - New beneficial effect of lansoprazole. *PLoS One*  
589 9, e97419. doi:10.1371/journal.pone.0097419.

590 Zhou, Y., Zhou, B., Pache, L., Chang, M., Khodabakhshi, A. H., Tanaseichuk, O., et al. (2019).  
591 Metascape provides a biologist-oriented resource for the analysis of systems-level datasets. *Nat.*  
592 *Commun.* 10, 1523. doi:10.1038/s41467-019-09234-6.

Zhu, H., Bouhifd, M., Donley, E., Egnash, L., Kleinstreuer, N., Kroese, E. D., et al. (2016). Supporting read-across using biological data. *ALTEX* 33, 167–182. doi:10.14573/altex.1601252.

Zhu, L., Roberts, R., Huang, R., Zhao, J., Xia, M., Delavan, B., et al. (2020). Drug repositioning for Noonan and LEOPARD syndromes by integrating transcriptomics with a structure-based approach. *Front. Pharmacol.* 11, 927. doi:10.3389/fphar.2020.00927.

## 10 Data Availability Statement

Publicly available datasets were analyzed in this study. This data can be found here: <https://toxico.nibiohn.go.jp/open-tggates/english/search.html>.

## 11 Figure Legends

**Figure 1.** Approach to construct a virtual microarray (RAID). The predictive model for comprehensive *in vivo* transcriptome data was constructed using elastic-net regression as well as chemical descriptors and *in vitro* transcriptome data.

**Figure 2.** PCA score plots for chemical substances and the gene loading in the transcriptome data of A) *in vivo*, B) virtual microarray (RAID), and C) *in vitro* data. PCA score plot with D) chemical descriptor data. Uppercase letters in PCA score plots: abbreviations of chemical substances are described in Tab.1. Color 1: non-toxic substances. Color 2: hepatotoxic substances. Gene symbols are presented on the arrowhead (loading).

613

614 **Figure 3.** List of genes that have high loading values in the PCA plot of *in vivo* data and their  
615 pathway map. The loading value was defined as the loading length in the 1<sup>st</sup> or 2<sup>nd</sup> quadrant  
616 calculated using the Pythagorean theorem. The pathway map was drawn by upstream regulator  
617 analysis using IPA.

618

619 **Figure 4.** Commonalities of principal components related genes and their biological functions  
620 analyzed by gene ontology and pathway analyses. Venn diagram of genes related to the 1<sup>st</sup> and 2<sup>nd</sup>  
621 principal components of *in vivo*, a virtual microarray (RAID), and *in vitro* data.

622

623 **Figure 5.** Enrichment analysis of *in vitro-in vivo* extrapolation (IVIVE) related genes identified in a  
624 virtual microarray (RAID) system. Top 20 most important (contribution) genes from the predictive  
625 models were analyzed.

626

627 **Figure 6.** Distribution of RMSEs of a virtual microarray (RAID) and *in vitro* data of A) all genes and  
628 B) *in vitro* genes having importance (contribution) in predictive models. \*\*p < 0.01 (Welch's *t*-test).

629

630 **Figure 7.** Read-across using PCA plot of external data predicted by a virtual microarray (RAID). A)  
631 *Cyp1a* and B) *Cyp4a* inducing chemical substances were analyzed for validation.

**Figure 1**

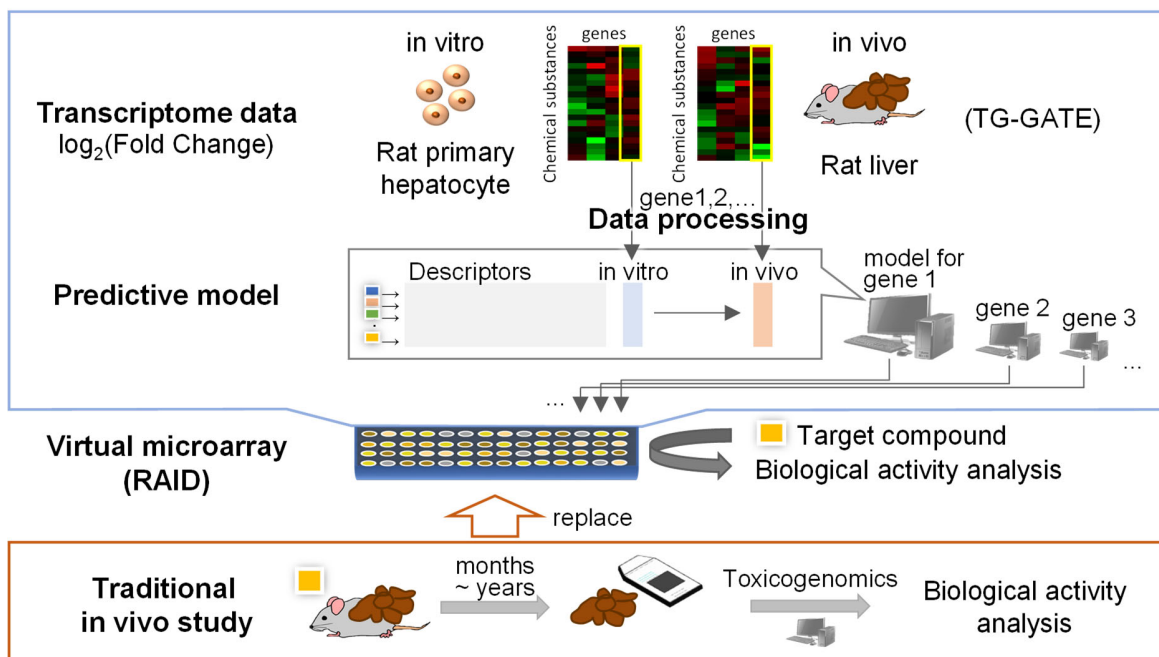


Figure 2

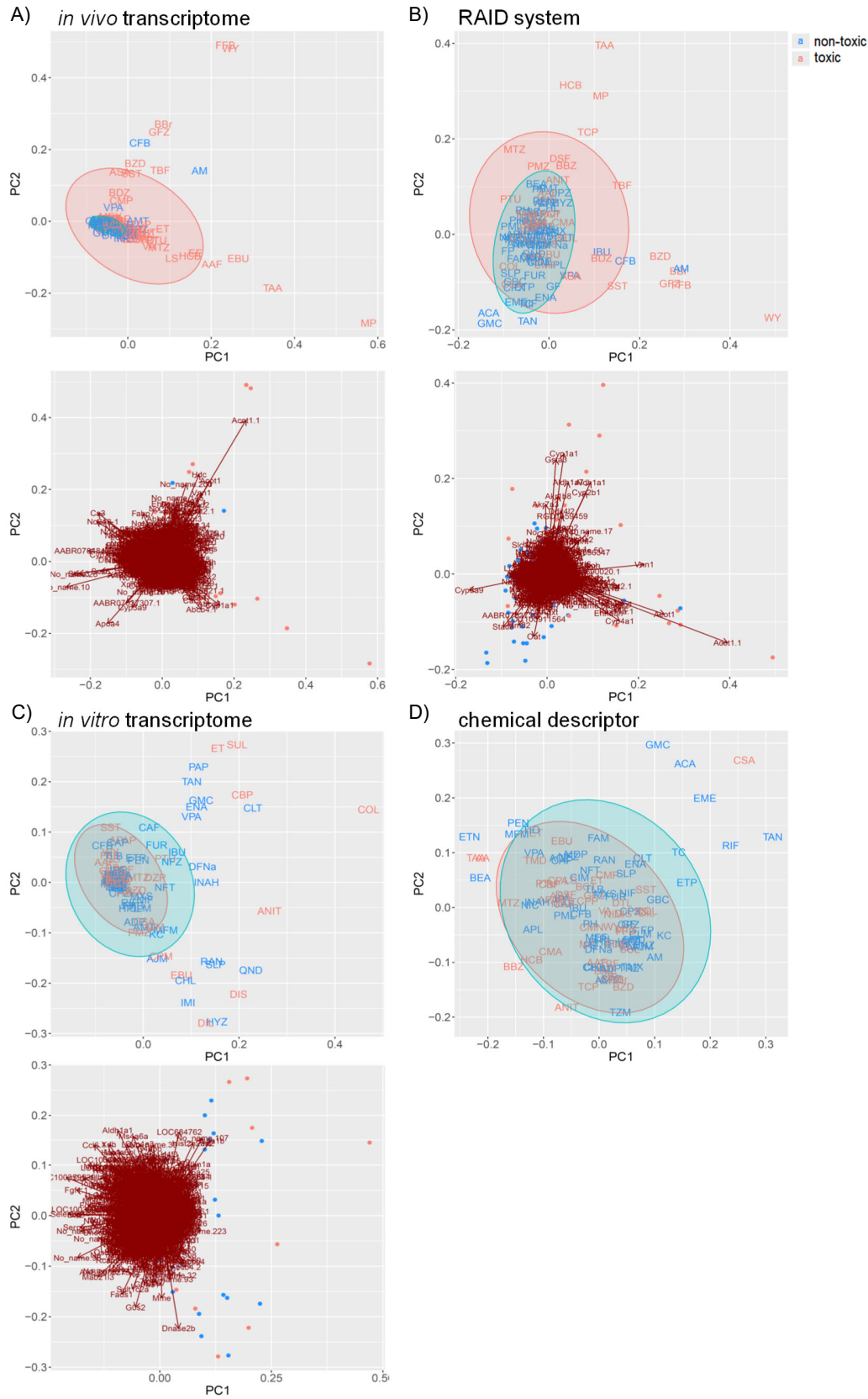
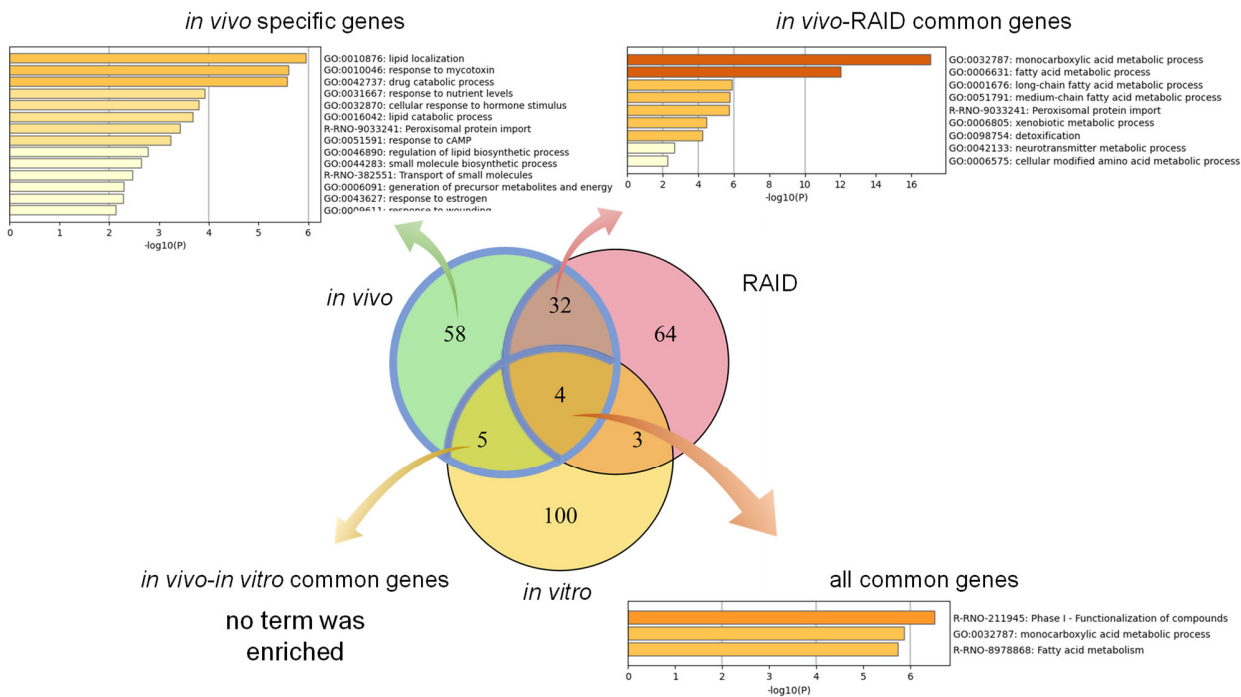


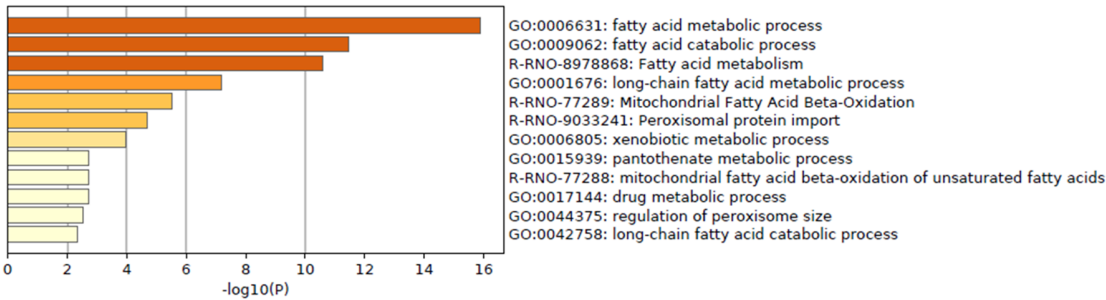




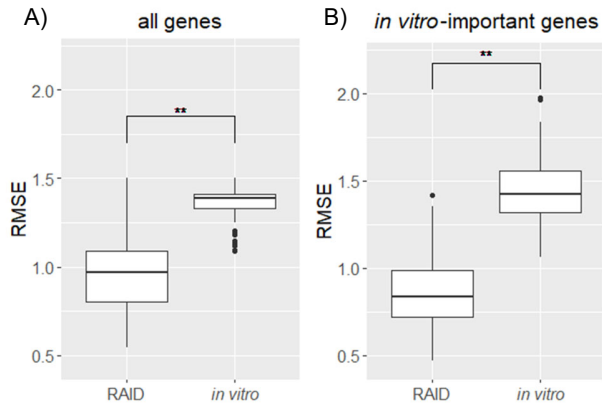
Figure 4



**Figure 5**



**Figure 6**





## 663 Tables

664 **Table 1.** List of compounds used in the present study and their toxicological classes.

Tox class <sup>1)</sup>	Compound name
Toxic	Allyl alcohol (AA), 2-acetamidofluorene (AAF), $\alpha$ -naphthyl isothiocyanate (ANIT), Acetaminophen (APAP), Aspirin (ASA), Benzbromarone (BBR), Bromobenzene (BBZ), Bucetin (BCT), Bendazac (BDZ), Benziodarone (BZD), carboplatin (CBP), Coumarin (CMA), Chlormezanone (CMN), Chloramphenicol (CMP), Colchicine (COL), Cyclophosphamide monohydrate (CPA), Clomipramine hydrochloride (CPM), Chlorpropamide (CPP), Cyclosporine A (CPA), Diltiazem hydrochloride (DIL), Disopyramide (DIS), Disulfiram (DSF), Dantrolene sodium hemiheptahydrate (DTL), Diazepam (DZP), Ethambutol dihydrochloride (EBU), 17- $\alpha$ -ethinylestradiol (EE), DL-ethionine (ET), Fenofibrate (FFB), Flutamide (FT), Gemfibrozil (GFZ), Hexachlorobenzene HCB), Lomustine (LS), Mexiletine hydrochloride (MEX), Methapyrilene hydrochloride (MP), Methyltestosterone (MTS), Methimazole (MTZ), Nimesulide (NIM), Phenacetin (PCT), Promethazine hydrochloride (PMZ), Propylthiouracil (PTU), Sulfasalazine (SS), Simvastatin (SST), Sulindac (SUL), Thioacetamide (TAA), Terbinafine hydrochloride (TBF), Ticlopidine hydrochloride (TCP), Trimethadione (TMD), Vitamin A (VA), WY-14643 (WY)
Non-toxic	Acarbose (ACA), Acetazolamide (ACZ), Adapin (ADP), Ajmaline (AJM), Amiodarone hydrochloride (AM), Amitriptyline hydrochloride (AMT), Allopurinol (APL), 2-bromoethylamine hydrobromide (BEA), Caffeine (CAF), Captopril (CAP), Carbamazepine (CBZ), Clofibrate (CFB), Chlorpheniramine maleate (CHL), Cimetidine (CIM), Chlormadinone acetate (CLM), Cephalothin sodium (CLT), Ciprofloxacin hydrochloride (CPX), Chlorpromazine hydrochloride (CPZ), Diclofenac sodium (DFNa), Danazol (DNZ), Erythromycin ethylsuccinate (EME), Enalapril maleate (ENA), Ethanol (ETN), Etoposide (ETP), Famotidine (FAM), Fluphenazine dihydrochloride (FP), Furosemide (FUR), Glibenclamide (GBC), Griseofulvin (GF), Gentamicin sulfate (GMC), Haloperidol (HPL), Hydroxyzine dihydrochloride (HYZ), Ibuprofen (IBU), Imipramine hydrochloride (IMI), Isoniazid (INAH), Iproniazid phosphate (IPA), Ketoconazole (KC), Methyldopa (MDP), Mefenamic acid (MEF), Metformin hydrochloride (MFM), Moxisylyte hydrochloride (MXS), Nitrofurantoin (NFT), Nitrofurazone (NFZ), Nicotinic acid (NIC), Nifedipine (NIF), Omeprazole (OPZ), Papaverine hydrochloride (PAP), Phenobarbital sodium (PB), D-penicillamine (PEN), Perhexiline maleate (PH), Phenylbutazone (PhB), Phenytoin (PHE), Pemoline (PML), Quinidine sulfate (QND), Ranitidine hydrochloride (RAN), Rifampicin (RIF), Sulpiride (SLP), Tannic acid (TAN), Tetracycline hydrochloride (TC), Tiopronin (TIO), Tolbutamide (TLB), Tamoxifen citrate (TMX), Triamterene (TRI), Thioridazine hydrochloride (TRZ), Triazolam (TXM), Sodium valproate (VPA)

1) The toxicological classes of chemical substances were referred to a previous report (Low et al., 2011). The authors classified these compounds into histopathological and serum chemistry classes. Compounds with hepatotoxic histopathological findings and other histopathological findings with biochemical marker changes in serum chemistry were defined toxic-compounds in this study.

**Table 2.** Principal components relating common genes in a virtual microarray (RAID) and *in vivo* data.

Probe ID	Symbol	Description
1398250_at	<i>Acot1</i>	Acyl-CoA thioesterase 1
1370269_at	<i>Cyp1a1</i>	Cytochrome P450, family 1, subfamily a, polypeptide 1
1387022_at	<i>Aldh1a1</i>	Aldehyde dehydrogenase 1, family member A1
1368934_at	<i>Cyp4a1</i>	Cytochrome P450, family 4, subfamily a, polypeptide 1
1388211_s_at	<i>Acot1</i>	Acyl-CoA thioesterase 1
1374070_at	<i>Gpx2</i>	Glutathione peroxidase 2
1367811_at	<i>Phgdh</i>	Phosphoglycerate dehydrogenase
1389253_at	<i>Vnn1</i>	Vanin 1
1388210_at	<i>Acot2</i>	Acyl-CoA thioesterase 2
1371089_at	<i>Gsta3</i>	Glutathione S-transferase alpha 3
1370491_a_at	<i>Hdc</i>	Histidine decarboxylase
1379275_at	<i>Snx10</i>	Sorting nexin 10
1370902_at	<i>Akr1b8</i>	Aldo-keto reductase, family 1, member B8
1367733_at	<i>Car2</i>	Carbonic anhydrase
1386889_at	<i>Scd2</i>	stearoyl-Coenzyme A desaturase 2

1386901_at	<i>LOC103690020</i>	Platelet glycoprotein 4-like
1391187_at	<i>Ppl</i>	Periplakin
1384225_at	<i>Dabl</i>	DAB adaptor protein 1
1384274_at	<i>AABR07037307</i>	similar to Spindlin-like protein 2
1395403_at	<i>Stac3</i>	SH3 and cysteine rich domain 3
1375845_at	<i>Aigl</i>	Androgen induced 1
1368283_at	<i>Ehhadh</i>	Enoyl-CoA hydratase and 3-hydroxyacyl CoA dehydrogenase
1387740_at	<i>Pex11a</i>	Peroxisomal biogenesis factor 11 alpha
1370067_at	<i>Me1</i>	Malic enzyme 1
1370870_at	<i>Me1</i>	Malic enzyme 1
1371886_at	<i>Crat</i>	Carnitine O-acetyltransferase
1379361_at	<i>Pex11a</i>	Peroxisomal biogenesis factor 11 alpha
1386885_at	<i>Ech1</i>	Enoyl-CoA hydratase 1
1367659_s_at	<i>Eci1</i>	Enoyl-CoA delta isomerase 1
1378169_at	<i>Acot3</i>	Acyl-CoA thioesterase 3
1374475_at	<i>Abhd1</i>	Abhydrolase domain containing 1
1387783_a_at	<i>Acaa1a</i>	Acetyl-Coenzyme A acyltransferase 1A
1390591_at	<i>Slc17a3</i>	Solute carrier, family 17, member 3
1368607_at	<i>Cyp4a8</i>	Cytochrome P450, family 4, subfamily a, polypeptide 8
1370698_at	<i>Ugt2b10</i>	UDP glucuronosyltransferase, family 2, member B10
1370387_at	<i>Cyp3a9</i>	Cytochrome P450, family 3, subfamily a, polypeptide 9

672

673

674

675

676 **Table 3.** List of top 20 genes with high importance *in vitro* data in the predictive models in RAID.

Probe ID	Symbol	Description	Importance of <i>in vitro</i> data
1398250_at	<i>Acot1</i>	Acyl-CoA thioesterase 1	0.549873
1368934_at	<i>Cyp4a1</i>	Cytochrome P450, family 4, subfamily a, polypeptide 1	0.411661
1367659_s_at	<i>Eci1</i>	Enoyl-CoA delta isomerase 1	0.35992
1368283_at	<i>Ehhadh</i>	Enoyl-CoA hydratase and 3-hydroxyacyl CoA dehydrogenase	0.348306
1387740_at	<i>Pex11a</i>	Peroxisomal biogenesis factor 11 alpha	0.313967
1370269_at	<i>Cyp1a1</i>	Cytochrome P450, family 1, subfamily a, polypeptide 1	0.284354
1386885_at	<i>Ech1</i>	Enoyl-CoA hydratase 1	0.251545
1389253_at	<i>Vnn1</i>	Vanin 1	0.243576
1387783_a_at	<i>Acaa1a</i>	Acetyl-Coenzyme A acyltransferase 1A	0.238282
1371076_at	<i>Cyp2b1</i>	Cytochrome P450, family 2, subfamily a, polypeptide 1	0.220351
1375845_at	<i>Aig1</i>	Androgen induced 1	0.166297
1388211_s_at	<i>Acot1</i>	Acyl-CoA thioesterase 1	0.126502
1379361_at	<i>Pex11a</i>	Peroxisomal biogenesis factor 11 alpha	0.125313
1386901_at	<i>LOC103690020</i>	Platelet glycoprotein 4-like	0.114874
1370397_at	<i>Cyp4a3</i>	Cytochrome P450, family 4, subfamily a, polypeptide3	0.11374
1386880_at	<i>Acaa2</i>	Acetyl-CoA acyltransferase 2	0.095809
1384244_at	<i>Hsd12</i>	Hydroxysteroid dehydrogenase like 2	0.074349
1370698_at	<i>Ugt2b10</i>	UDP glucuronosyltransferase, family 2, member B10	0.073172
1397468_at	<i>Hsd12</i>	Hydroxysteroid dehydrogenase like 2	0.07087
1367777_at	<i>Decr1</i>	2,4-dienoyl-CoA reductase 1	0.069522



677 **Table 4.** List of chemical substances used for external validation of RAID system.

Name	CAS No.	Name in PCA plot
<i>Potential Cyp1a inducers</i>		
2,3,4,7,8-pentachlorodibenzofuran	57117-31-4	Pentachlorodibenzofuran
3,4,5,3',4'-pentachlorobiphenyl	57465-28-8	Pentachlorobiphenyl
3-methylcholanthrene	56-49-5	Methylcholanthrene
9,10-dimethyl-1,2-benzanthracene	57-97-6	Dimethylbenzanthracene
Benzo(a)pyrene	50-32-8	Benzo(a)pyrene
Dexamethasone	8054-59-9	Dexamethasone
Genistein	446-72-0	Genistein
2,2',4,4'-tetrachlorobiphenyl	1336-36-3	Tetrachlorobiphenyl
Quercetin	117-39-5	Quercetin
Resveratrol	501-36-0	Resveratrol
Thiabendazole	148-79-8	Thiabendazole
<i>Potential Cyp4a inducers</i>		
Streptozotocin	18883-66-4	Streptozotocin
2-ethylhexanol	104-76-7	Ethylhexanol
Di(2-ethylhexyl) phthalate	117-81-7	Di(2-ethylhexyl)_phthalate
Clofenapate	21340-68-1	Clofenapate
Clofibric acid	882-09-7	Clofibric_acid
Ciprofibrate	52214-84-3	Ciprofibrate
Nafenopin	3771-19-5	Nafenopin
TO-901317	293754-55-9	TO-901317

Acetaminophen	719293-04-6	Acetaminophen
Diltiazem	33286-22-5	Diltiazem

---

678